

HP HIERARCHICAL ADAPTIVE FORMULATION FOR THE BOUNDARY INTEGRAL METHOD APPLIED TO A STOKES FLOW: A PROPOSAL

Raul Bernardo Vidal Pessolani

School of Engineering, Fluminense Federal University
R. Passos da Pátria 156, bl.D, sl.407, Niterói, R.J, Brazil.
CEP: 24210-240. E-mail: raul@mec.uff.br

Roger Matsumoto Moreira

School of Engineering, Fluminense Federal University
R. Passos da Pátria 156, bl.D, sl.505, Niterói, R.J, Brazil.
CEP: 24210-240. E-mail: rmmoreira@engenharia.uff.br

Abstract. A boundary integral method with an HP hierarchical adaptive formulation applied to a Stokes flow problem is proposed. This work was motivated by previous results in which a large number of discretization points were necessary in order to compute accurate solutions (Moreira & Teles da Silva 1997). The use of an adaptive scheme can reduce significantly the size of the grid and the computational demand required, with a significant reduction of the CPU time for a certain numerical error. This is highly recommended, especially in a transient free surface flow, where for each time-step a new solution has to be determined. The preliminary results show that the HP adaptive technique represents an efficient tool to study free surface flow problems since it can resolve regions of high curvature more accurately.

Keywords. Creeping flows, free surface flows, boundary integral method.

1. Introduction

Many problems in fluid mechanics involve low Reynolds number flows with free surfaces or rigid interfaces, also known as Stokes or creeping flows. These flows are governed by the Stokes equation, in which inertia forces are negligible compared to viscous and pressure forces. Industrial applications include the effect of surface roughness on lubrication, coating and extrusion operations. In natural systems, low Reynolds number flows are important in biomedical applications (e.g. air flow in small lung cavities) and in studies of microorganisms locomotion. In a larger length scale, the plastic deformation of rocks in the Earth's mantle and the mountain building process are geophysical phenomena in which viscosity plays an important role. The continuous continental drift of Earth's crust produces mixing and sediment transport to lower layers. The brittle material that composes the basis of the lithosphere and the uppermost asthenosphere is misshapened when submitted to high temperatures and pressures for a long period of time and thus can be considered as a viscous fluid flowing at low Reynolds number.

Modelling an unsteady viscous free surface flow is a difficult task to deal with since these problems are highly nonlinear, requiring special mathematical treatment. Under certain conditions asymptotic solutions for flows that deviate slightly from known simple configurations can be found. However numerical techniques such as boundary-integral, finite-difference and finite-element formulations are more flexible and have been employed in the solution of problems with different geometries. Finite-difference and finite-element methods have the disadvantages of intersecting the free surface with their underlying grid and in general require large computational efforts. The boundary integral method reduces significantly the computational demand for the calculation of the fluid motion since only surface properties are evaluated, with accurate nonlinear solutions for the free surface flow.

The present work aims to investigate the free surface flow induced by the displacement of a rigid impermeable plate with a well-defined geometry over a fluid with very high viscosity (see figure 1). This work is motivated by previous natural observations and experimental works in which interesting features occurring at the free surface were reported (Jeong & Moffatt 1992, Moreira 1997). The transient Stokes flow resulting from the translation of the rigid slab is modelled and solved via a boundary integral equation based on Lorentz reciprocal theorem (Higdon 1985, Pozrikidis 1988). The resultant free surface flow shows that a large number of discretization points are required in order to compute accurate solutions for the boundary values of stress and velocity (Moreira & Teles da Silva 1997). An adaptive formulation applied to this problem can reduce significantly the final system of equations and its computational demand, while the use of an iterative solver is also recommended in order to reduce the time of convergence of the solution. A better discretization of the regions of high curvature can then be achieved with the adaptive formulation.

Several articles have been published showing applications of the adaptive technique with an hierarchical formulation to potential flow problems (Pessolani 1989) and elasticity (Kita *et al.* 2000, Pessolani 2002). The H formulation is applied to elements where the expected solution tends to be asymptotic. It increases the number of discretization points inside each element and converges exponentially. The P formulation increases the order of the interpolation function and is indicated where the expected solution is smooth. It converges exponentially on the elements, but on the other elements it has problems of convergence. According to Zienkiewicz & Zhu (1989), for the finite element method the H formulation gives for linear and quadratic functions an accuracy of 5 to 10% measured in the global energy norm, being especially efficient for quadratic functions. However, when a higher accuracy is required, the P or HP formulation is necessary. In the present work an hierarchical P formulation associated with an H procedure is proposed aiming to optimize the resolution of the boundaries, especially at regions of high curvature.

This paper aims to introduce the application of a hierarchical adaptive boundary formulation to a Stokes flow problem. First the boundary value problem and the method of solution are defined. Then the hierarchical HP adaptive boundary element formulation is introduced and the singularity of the fundamental solution is discussed in order to perform the hierarchical formulation. To control the adaptive process, an error indicator is used based on the residual interpolation inside the element. At present the numerical code is under development but some examples with an equally spacing mesh are reviewed, illustrating the applicability of the method.

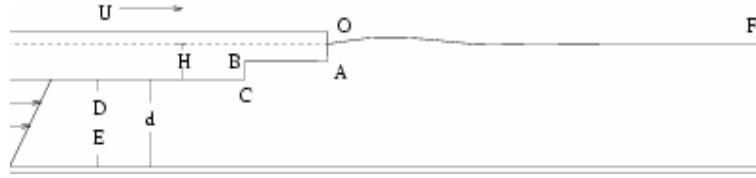


Figure 1. A sketch of the geometry in study (Moreira & Teles da Silva 1997).

2. Boundary value problem

Figure (1) illustrates the flow produced by the impulsive motion of a rigid indented slab, suddenly accelerated from rest to a constant horizontal velocity U of 5 cm/yr, over a deep layer of fluid. The slab sinks into the fluid for a depth H of 40 km, which is less than its total height. As a typical case we consider the fluid with a kinematic viscosity μ of 4×10^{19} kg/ms and a density ρ of 3.2 g/cm³. The large difference in magnitude of these quantities poses difficulties for obtaining accurate numerical results; though, this problem can be solved through the introduction of convenient length, mass and time scales. We thus define the submerged thickness H , the velocity of the slab U and the fluid density ρ , respectively, as the length, velocity and density units. With these definitions, time can be measured in terms of H/U u.t. ($\cong 0.8$ m.y.), accelerations in terms of $\mu U / (\rho H^2)$ u.a. ($\cong 12.4$ m/s²) and stresses in terms of $\mu U / H$ u.s. ($\cong 1.6$ MPa). These values produce a Reynolds number equal to,

$$\text{Re} = \frac{\rho H U}{\mu} \cong 10^{-21},$$

which is small enough to allow the hypothesis of Stokes flow to be valid for length scales of thousands of kilometers. As a two-dimensional model we enclose the flow within two rigid boundaries i.e. segment EF , such that we obtain a solution valid for the whole domain (Happel & Brenner 1965, section 2.7). We are interested in deep fluid layers with large values of d ($\cong 400$ km), which include the lithosphere, the asthenosphere and part of the mesosphere, and in large horizontal extensions of the free surface, extending it for many depths d of length.

The velocity field \vec{u} and the pressure p must satisfy the following dimensionless equations in the whole fluid domain,

$$\nabla \cdot \vec{u} = 0, \quad -\nabla p + \vec{g} + \nabla^2 \vec{u} = 0. \quad (1)$$

The first equation represents the continuity equation and the last one is the Stokes equation. The boundary conditions for the flow field are given in terms of the velocity \vec{u} and the stress \vec{f} , where in Einstein's notation,

$$f_i = \left[-p \delta_{ij} + \mu \left(\frac{\partial u_i}{\partial x_j} + \frac{\partial u_j}{\partial x_i} \right) \right] n_j. \quad (2)$$

The contour of the fluid domain is formed by four different surfaces, each of them with distinct boundary conditions, as described below.

- i) The free surface is represented by the segment FO , where the tangential component of the stress is equal to zero and its normal component assumes the value of a reference pressure p_0 exerted by material lying above this surface. With no loss of generality, we suppose that this pressure has a constant value $p_0 = 0$. So the stress condition on the free surface becomes $\vec{f} = (0, 0)$. Note that on this contour the velocity \vec{u} is unknown.
- ii) The segmented line OD corresponds to the contour of the rigid slab in contact with the fluid, where both conditions of impenetrability and no-slipping must be satisfied, so that $\vec{u} = (U, 0)$. The components of stress \vec{f} are the unknown in this region.
- iii) The vertical stretch DE is supposed to be far from the right end of the rigid slab. At this region the flow between two parallel and infinite flat plates is used as an approximation, the upper plate moving with a constant velocity U while the

bed is at rest. The velocity profile is thus linear, given by $\bar{u}=(U(1+(H+y)/d),0)$, where $-(d+H)\leq y\leq -H$. The stress at this region can be easily determined by substituting the linear velocity profile into equation (2), giving $\bar{f}_i=(\mu U/d)\omega_j n_j$, where,

$$\omega_j = \begin{bmatrix} 0 & 1 \\ 1 & 0 \end{bmatrix}$$

iv) The stretch EF is formed by a horizontal rigid floor and a vertical wall. In this region the no-slip and impenetrability conditions are valid i.e. $\bar{u}=(0,0)$, and the stress \bar{f} has to be determined.

The boundary value problem described by the system of equations (1) and the boundary conditions above does not involve time derivatives. Though, this is a time evolution problem where the velocity field is determined by the total derivative of the fluid particle's position. At any time the free surface flow is conditioned by the geometry of its boundaries and by the conditions imposed on them, characterizing a *quasi-static* process (Happel & Brenner 1965). Then the time evolution of the flow can be determined by an Eulerian scheme,

$$\bar{x}(\xi, t+\Delta t) = \bar{x}(\xi, t) + \bar{u}(\xi, t)\Delta t + O(\Delta t^2), \quad (3)$$

where ξ is the parameter describing the contour of the free surface and Δt is the time interval used in the numerical computations.

To simplify the application of the boundary integral method to the Stokes flow problem, gravity is transferred from the governing equations to the boundary conditions (Pozrikidis 1988). A change in the sign of the boundary conditions produces a reversal in the velocity and stress fields for the same partial differential equations governing the phenomenon, and also guarantees the reversibility of the flow (Taylor 1963). This procedure also simplifies the application of the dynamic boundary condition on the free surface. Therefore the flow is decomposed into a basic one, represented by \bar{u} , and a disturbed flow, described by \bar{u}' . We can thus represent the velocity and stress fields by,

$$\bar{u} = \bar{u} + \bar{u}', \quad \bar{f} = \bar{f} + \bar{f}'. \quad (4)$$

The basic flow is supposed to be null in all the fluid domain i.e. $\bar{u}'=(0,0)$, with the ‘‘hydrostatic’’ stress applied at all contours given by $\bar{f}' = -(\bar{g} \cdot \bar{x})\bar{n}$, satisfying the Stokes equation. The disturbed flow with solutions \bar{u}' and \bar{f}' must satisfy,

$$\nabla \cdot \bar{u}' = 0, \quad -\nabla p' + \nabla^2 \bar{u}' = 0, \quad (5)$$

where the boundary conditions expressed in terms of the perturbed velocity \bar{u}' are identical to those associated to the main problem shown in items (ii), (iii) and (iv) of this section. This occurs because $\bar{u}'=(0,0)$, and from expression (4), we have $\bar{u} = \bar{u}'$. The boundary conditions relative to the perturbed stress \bar{f}' differ from the main problem by the absence of the ‘‘hydrostatic’’ pressure contribution. Substituting the previous expressions of \bar{f} and \bar{f}' in equation (4), we obtain the boundary condition for \bar{f}' at the free surface: $\bar{f}' = (\bar{g} \cdot \bar{x})\bar{n}$. In this way \bar{g} is introduced into the main problem. Note that the sum of the basic and disturbed stresses satisfies the boundary condition applied at the free surface in the main problem. The boundary condition in terms of the stress is also modified in the stretch DE , becoming $\bar{f}'_i = (\mu U/d)\omega_j n_j$. So we now have to determine \bar{u}' and \bar{f}' which satisfy the system of equations (5) and the boundary conditions summarized above.

3. Boundary integral solver

The disturbed flow is solved in a dimensionless form through the use of a boundary integral equation of the form (Higdon 1985),

$$\bar{u}'_i(\bar{x}_m) = \frac{1}{2\pi} \left\{ \int_S \left[\ln(r) \bar{f}'_i(\bar{x}_n) - \frac{r_i r_j}{r^2} \bar{f}'_j(\bar{x}_n) - 4 \frac{r_i r_j r_k}{r^4} \bar{u}'_k(\bar{x}_n) n_k \right] dS \right\}, \quad (6)$$

where $i, j, k = 1, 2$; $\bar{\bar{u}}$ and $\bar{\bar{f}}$ are respectively the disturbed velocity and stress on the boundary of the domain; \bar{n} is the unit normal vector pointing out of the fluid; \bar{x}_m and \bar{x}_n give the position of the fluid particles; $r_i = \bar{x} - \bar{x}_m$; $r = |r_i|$. For the velocity field $\bar{\bar{u}}$ inside the fluid domain, the factor $1/2\pi$ is replaced by $1/4\pi$.

The numerical solution is obtained through a discretization of the boundaries of the fluid domain. A set of points \bar{x}_m is evenly distributed along the contour and interpolated by quadratic functions for the variables \bar{x} , $\bar{\bar{u}}$ and $\bar{\bar{f}}$. Hence, the integral equation (6) is approximated by a system of linear equations, whose unknowns are the disturbed stresses $\bar{\bar{f}}$ at the rigid boundaries and the perturbed velocities $\bar{\bar{u}}$ at the free surface. The solution of the main problem is given by the sum of the disturbed and unperturbed flows. The free surface motion is determined by equation (3).

Using natural cubic splines with an equally spacing grid, Moreira & Teles da Silva (1997) showed that a large number of discretization points are required in order to solve accurately the final system of equations. Using a Cray J90 of NACAD/COPPE/UFRJ, they computed 12 time-steps corresponding to 5.2 m.y. with a total CPU time of 9,000 seconds. Due to limitations of computational resources, longer runs were not possible. In the next sections an HP hierarchical adaptive formulation with iterative solvers is introduced aiming to reduce the size of the system of equations and the time of convergence of the solution.

4. HP hierarchical adaptive formulation

The adaptive scheme is an iterative process which aims to find out the best mesh applied to a certain problem. The rational way to compute the process is to store the information from one iteration to the following, incorporating only the new refined computation. This procedure is called hierarchical and was introduced by Parreira & Dong (1992). This means that in a new iteration it is not necessary to compute again all the coefficients for the old and new collocation points. This is necessary for the adaptive process where several discretizations are necessary until the correct solution is reached. To make it possible, the H formulation uses hierarchical families of interpolation functions. Those functions are accumulative i.e. the higher order functions are generated without modifying lower order contributions. In the subsequent discretization, the new system is set up increasing the previous system with sub matrices A_{12} , A_{21} , A_{22} and the vector b_2 , corresponding to the new collocation points as shown below.

$$\begin{bmatrix} \boxed{A_{11}} & \boxed{A_{12}} \\ \boxed{A_{21}} & \boxed{A_{22}} \end{bmatrix} \begin{bmatrix} \boxed{x_1} \\ \boxed{x_2} \end{bmatrix} = \begin{bmatrix} \boxed{b_1} \\ \boxed{b_2} \end{bmatrix} \quad (7)$$

The idea is to include intermediate collocation points in the element, with interpolation functions of the same order of the previous points which can be conventional Langrangians. For a quadratic interpolation, it is defined a set of interpolation functions N_2 such that,

$$N_{2,kl} = \begin{cases} 0 & \text{if } |\eta - \eta_{2l}| \geq D_\eta/k \\ 1 - \frac{(\eta - \eta_{2l})^2}{\left(\frac{D_\eta}{k}\right)^2} & \text{if } |\eta - \eta_{2l}| \leq D_\eta/k \end{cases} \quad (8)$$

D_η is half of the element to be refined in natural coordinates, k is the requested number of divisions, while η_{11} and η_{21} are the natural coordinates of the nodes used, respectively, in the linear and quadratic interpolations. For each degree λ , $2^{\lambda-1}$ bubble functions are generated with the corresponding collocation points arranged symmetrically, equally spaced along the element. Figure 2 shows the collocation points in a second level of hierarchical discretization.

The approximate solution $\hat{\varphi}$ on the element is expressed in terms of the previous and the new values on the nodes,

$$\hat{\varphi} = \sum_{c=0}^2 N_c(\xi) \hat{\varphi}_c + \sum_{c=3}^4 N_c(\xi) \hat{\varphi}_c \quad (9)$$

For an iteration λ , we suppose A the number of hierarchical levels and Π_λ the list of integers indicating which pair of hierarchical functions Π is applied in the mesh (for each level λ , there are $2^{\lambda-1}$ pairs). The approximate solution is then

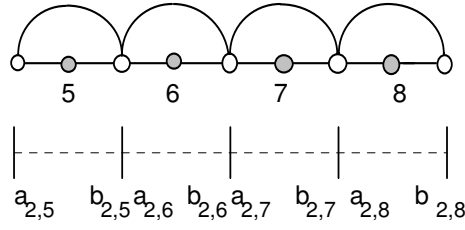


Figure 2. Second level of hierarchical discretization.

given by,

$$\hat{\alpha}(\eta) = \sum_{c=0}^2 N_c(\eta) \hat{\phi}_c + \sum_{\lambda=1}^{\Lambda} \sum_{k \in \Pi_{\lambda}} [N_{\lambda,2k-1}(\eta) \hat{\phi}_{\lambda,2k-1} + N_{\lambda,2k}(\eta) \hat{\phi}_{\lambda,2k}]. \quad (10)$$

At the iteration λ ,

$$N_{\lambda,n} = \begin{cases} N_{\lambda,2}(t_{\lambda,n}(\eta)) & \text{for } \eta \in [a, b]_{\lambda,n}, \\ 0 & \text{otherwise} \end{cases}, \quad (11)$$

where,

$$a_{\lambda,n} = -1 + (n-1) \frac{1}{2^{(\lambda-1)}}, \quad (12)$$

$$b_{\lambda,n} = a_{\lambda,n} + \frac{1}{2^{(\lambda-1)}}.$$

$t_{\lambda,n}$ is the natural coordinate mapped in the interval $[a_{\lambda,n}, b_{\lambda,n}]$ defined by,

$$t_{\lambda,n}(\eta) = 2^{\lambda}(\eta + 1) - 2n + 1. \quad (13)$$

For the P formulation, Legendre integrated polynomials are used, with a good numerical stability when applied to elliptical problems. Let the Legendre polynomials be,

$$N_0(\eta) = \frac{1-\eta}{2}; N_1(\eta) = \frac{1+\eta}{2}; N_i(\eta) = \phi_i(\eta), \quad i = 2, 3, \dots, p+1, \quad (14)$$

where ϕ_i is defined in term of the Legendre polynomials P_{i-1} ,

$$\phi_i(\eta) \stackrel{\text{def}}{=} \sqrt{\frac{2i-1}{2}} \int_{-1}^{\eta} P_{i-1}(t) dt \quad \text{where } i = 2, 3, \dots \quad (15)$$

which integrated yields to,

$$\phi_i(\eta) = \frac{1}{\sqrt{2(2i-1)}} (P_i(\eta) - P_{i-2}(\eta)). \quad (16)$$

The interpolation functions of the integrated polynomials are:

$$N_2 = \phi_2(\eta) = \frac{3}{2\sqrt{6}} (\eta^2 - 1), \quad (17)$$

$$N_3 = \phi_3(\eta) = \frac{5}{2\sqrt{10}} (\eta^3 - \eta), \quad (18)$$

$$N_4 = \phi_4(\eta) = \frac{7}{8\sqrt{14}} (5\eta^4 - 6\eta^2 + 1), \quad (19)$$

$$N_5 = \phi_5(\eta) = \frac{9}{8\sqrt{18}}(7\eta^5 - 10\eta^3 + 3\eta), \quad (20)$$

$$N_6 = \phi_6(\eta) = \frac{11}{16\sqrt{22}}(21\eta^6 - 35\eta^4 - 15\eta^2 - 1). \quad (21)$$

The HP strategy is shown in figure 3. The initial system is composed by Lagrangian quadratic functions. After solving the system, the routines are executed and an error indicator is applied to evaluate the solution accuracy. If a new regrid is required, collocation points are generated with new interpolation functions and added to the original matrix system. This process is repeated until the requested precision is achieved or a bad condition appears.

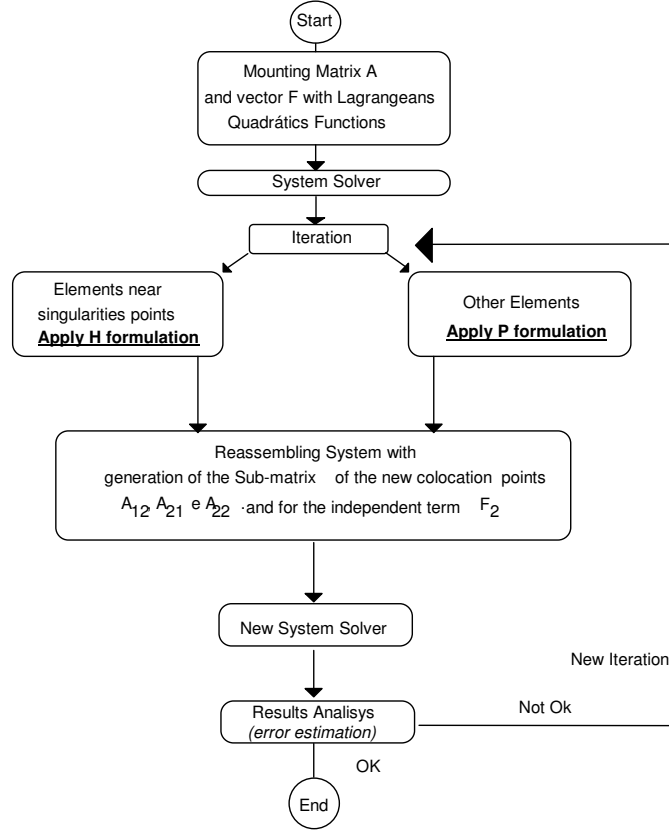


Figure 3. The HP adaptive scheme.

5. Singular terms in the boundary integral equation

From the boundary integral equation (6) it is possible to find out that the fundamental solutions T^* and U^* are of the form (Higdon 1985, Pozrikidis 1988),

$$T_{ij}^*(\xi, \chi) = \frac{-1}{4\pi(1-\nu)r} \left[(1-2\nu)\delta_{ij} + 2r_{,i}r_{,j} \right] \frac{\partial r}{\partial n} - (1-2\nu)(r_{,i}n_{,j} - r_{,j}n_{,i}), \quad (22)$$

$$U_{ij}^*(\xi, \chi) = \frac{-1}{8\pi(1-\nu)G} \left[(3-4\nu)\ln(r)\delta_{ij} - r_{,i}r_{,j} \right]$$

The use of the hierarchical formulation depends on the computation of the singular terms. When the source point coincides with the field point, $r \rightarrow 0$, and thus some of the terms may require special treatment since they become singular of $1/r$ and $\ln(r)$ orders. The numerical computation of these integrals can be highly imprecise depending on the method used. $\ln(r)$ singularity can be numerically integrated by Gauss, but it demands a great number of points and the use of Telles (1987) transformation to re-map the integration points. On the other hand, singularities of $1/r$ order require the integration with respect to Cauchy's principal value. Usually the solution in elasticity consists in computing these terms as rigid body displacements. However, these singular integrals may be directly estimated.

The exact computation of the indicated integrals can be done by analytical procedures. However, expressions may become too complex in curved elements. So the semi-analytical integration presented by Pessolani (1997) is recommended. The numerical expression for the term $1/r$ then becomes,

$$I_G = \left\{ \int_{-1}^1 \left[F'_d(\eta) \left| \frac{d\Gamma(\eta)}{dr} \right| - F'_d(\xi) \right] \ln r \left| \frac{dr(\eta)}{d\eta} \right| d\eta + F'_d(\xi) \cdot r_f (\ln(r_f) - 1) \right\} \\ + \left\{ \int_{-1}^1 \left[F'_d(\eta) \left| \frac{d\Gamma(\eta)}{dr} \right| - F'_d(\xi) \right] \ln r \left| \frac{dr(\eta)}{d\eta} \right| d\eta + F'_d(\xi) \cdot r_i (\ln(r_i) - 1) \right\} \quad (23)$$

The $\ln(r)$ term is computed similarly by,

$$I_H = \int_{-1}^1 \frac{1}{r} \left(F_d(\eta) \left| \frac{d\Gamma(\eta)}{dr} \right| - F_d(\xi) \right) \left| \frac{dr(\eta)}{d\eta} \right| d\eta + F_d(\xi) \ln(r_d) + \\ + \int_{-1}^1 \frac{1}{r} \left(F_a(\eta) \left| \frac{d\Gamma(\eta)}{dr} \right| - F_a(\xi) \right) \left| \frac{dr(\eta)}{d\eta} \right| d\eta + F_a(\xi) \ln(r_d) \quad (24)$$

where for the \ln term, $F'_d = (1/2\pi)\delta_{ij}$, and for the $1/r^d$ term, $F' = (1/2\pi)4r_i r_j r_k n_k$. Some precautions have to be taken when the source point is inside the element field. In this case it is advisable to divide the element by two, before and after the point, and perform the integration separately.

6. Error estimates

The error indicator gives the information about its size while the error estimator makes the control of the adaptive process, indicating the global error. Parreira's (1992) indicator is used in our formulation, based on the calculation of the residue inside the element. The process is represented in figure 4. Parreira's indicator and estimator have the advantage of using the hierarchical terms directly, saving CPU time. It is more direct than others and have good results.

7. Iterative solvers

Iterative solvers can improve the solution of the adaptive process and become significantly efficient when running many iterations with a dimension of the system equations greater than 200 (Pessolani 1999). To increase the convergence ratio, the initial solution of the next iteration takes the form of the final solution of the last iteration. The tolerance can be less accurate (1.e-3), accurate (1.e-6) or more accurate (1.e-10). In our formulation, the algorithm GMRES developed by Shakib & Hughes (1989) is used. The Krylov sub-space has to be fixed in order to represent the vector solution. If it is super dimensioned, it will occupy a considerable memory space; however in another way it could not give the correct answer. It is important to find out the ideal point to give good results with a rational computer range.

8. Preliminary results

Figure (5) shows the tangential and normal stresses at the horizontal stretch AB when the slab moves forward ($U > 0$), supposing a discretization by natural cubic splines with an equally spacing grid of $0.25 H$. Figure (5a) shows a change of sign in the tangential stress, which may denote the existence of a reverse flow near the point B . If that is the case an eddy may be formed in this region. Moffatt (1964) shows that a sequence of eddies of decreasing size and intensity is formed near a corner in a Stokes flow, even in the presence of a free surface. These eddies can have an important role in the transport of sediments between different layers of the lithosphere and asthenosphere. The existence of peaks near the corners A and B were also reported by Higdon (1985). At these regions an abrupt change of the slope inserts a strong geometry discontinuity. The use of an HP adaptive formulation can certainly help to investigate this phenomenon more accurately since the point B is located in a region of high curvature which is poorly resolved. Another feature observed in figure (5b) is the growth of the positive normal stress with time when the slab moves forward. These stresses tend to lift the front of the rigid slab. After a short period of time (0.5 u.t.) the normal stress is fully dominated by the "hydrostatic" force induced by the gravitational field. However, after 3.5 u.t. the contribution of the unsteady flow starts to appear when the normal stresses assume positive values.

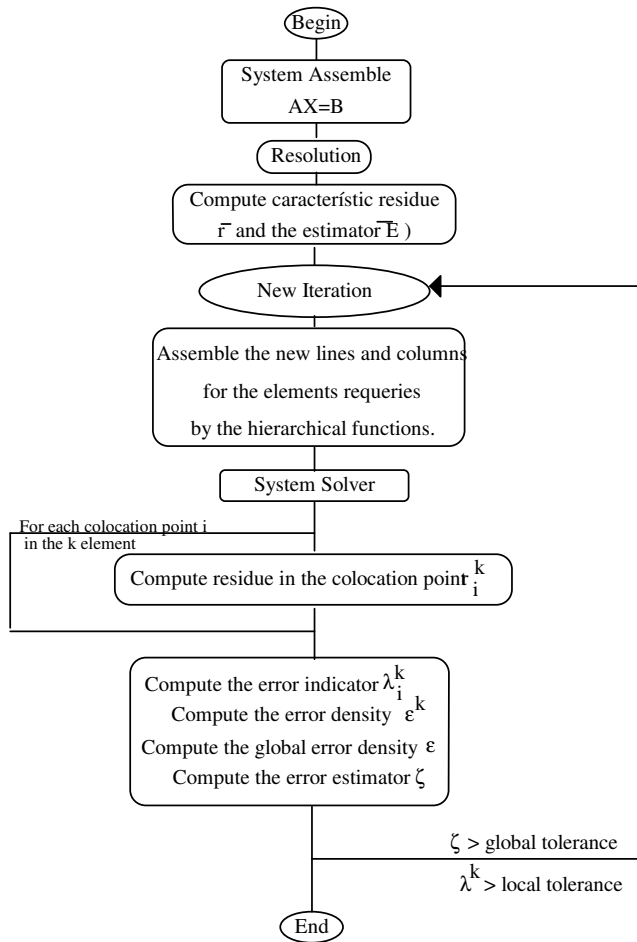


Figure 4. Parreira's indicator and estimator.

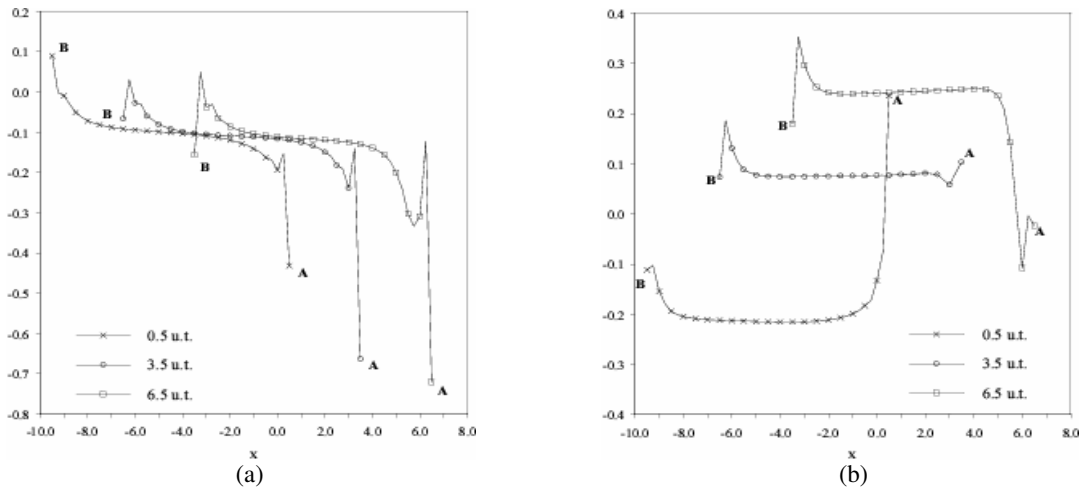


Figure 5. (a) Tangential and (b) normal stress distribution at the horizontal stretch AB for $U>0$; the grid points have a spacing of $0.25 H$ (Moreira & Teles da Silva 1997).

9. Conclusions

A boundary integral method with an HP hierarchical adaptive formulation applied to a Stokes flow problem is proposed. This work was motivated by previous results in which a large number of discretization points were necessary in order to compute accurate solutions (Moreira & Teles da Silva 1997). The use of an adaptive scheme can reduce

significantly the size of the grid and the computational demand required, with a significant reduction of the CPU time for a certain numerical error. This is highly recommended, especially in a transient free surface flow, where for each time-step a new solution has to be determined. The preliminary results show that the HP adaptive technique represents an efficient tool to study free surface flow problems since it can resolve regions of high curvature more accurately.

10. Acknowledgement

We acknowledge the fruitful discussions with Dr. A.F. Teles da Silva (PEM/COPPE/UFRJ) and Dr. W.J. Mansur (PEC/COPPE/UFRJ).

11. References

- Happel, J. & Brenner, H., 1965, "Low Reynolds Number Hydrodynamics with Special Applications to Particulate Media." 1st ed., New Jersey, Prentice-Hall, Inc.
- Higdon, J.J.L., 1985, "Stokes flow in arbitrary two-dimensional domains: shear flow over ridges and cavities." *Journal of Fluid Mechanics*, v. 159, pp. 195-226.
- Jeong, J.-T. & Moffatt, H.K., 1992, "Free surface cusps associated with flow at low Reynolds number." *Journal of Fluid Mechanics*, v. 241, pp. 1-22.
- Moffatt, H.K., 1964, "Viscous and resistive eddies near a sharp corner." *Journal of Fluid Mechanics*, v. 18, pp. 1-18.
- Moreira, R.M., 1997, "Simulação numérica do escoamento de Stokes com superfície livre sob uma placa rígida." *Dissertação de mestrado, PEM/COPPE/UFRJ, Brazil.*
- Moreira, R.M. & Teles da Silva, A.F., 1997, "Modelagem da tectônica de placas na crosta terrestre." *Anais do XIV COBEM, Bauru*, pp. 1-8.
- Kita, E., Higuchi, K.E. & Kamiya, N., 2000, "Application of r and hr-adaptive BEM to two-dimensional elastic problems." *Engng. Analysis with Boundary Elements*, 24, pp. 317-324.
- Parreira, P. & Dong, Y.F., 1992, "Adaptive Hierarchical Boundary Elements." *Advances in Engng. Software*, pp. 249-259.
- Pessolani, R.B.V., 1989, "Formulação H auto adaptativa de elementos de contorno para problemas de potencial e elasticidade." *Dissertação de Mestrado, PUC-RJ.*
- Pessolani, R.B.V., 1997, "Semi-analytical singular integration for the boundary element method for elasticity." *Anais do XIV COBEM, Bauru.*
- Pessolani, R.B.V., 1999, "Utilização de Solvers Iterativos em Programas Adaptativos Hierárquicos no Método dos Elementos de Contorno." *Anais do XV COBEM, Campinas.*
- Pessolani, R.B.V., 2002, "An HP-Adaptive Hierarchical Formulation for the Boundary Element Method Applied to Elasticity in Two Dimensions." *Revista Brasileira de Ciências Mecânicas*, v. 24, pp. 1-9.
- Pozrikidis, C., 1988, "The flow of a liquid film along a periodic wall." *Journal of Fluid Mechanics*, v. 188, pp. 275-300.
- Shakib, F., Hughes, J.R., 1989, "A multi-element group preconditioned GMRES algorithm for nonsymmetric systems arising in finite element analysis." *Comp. Meth. in Appl. Mech. & Engng.*, 75, pp. 415-456.
- Taylor, G.I., 1963, "Low Reynolds Number Flow." *Encyclopaedia Britannica Educational Corporation, 21617 EN VHS, Britannica.*
- Telles, J.C.F., 1987, "A self-adaptive coordinate transformation for efficient numerical evaluation of general boundary element integrals." *Int. J. Num. Meth. Engng.*, 24, pp. 952-973.
- Zienkiewicz, O.C. & Zhu, J.Z., 1989, "A simple error estimator and adaptive procedure for practical engineering analysis." *Int. J. Num. Meth. Engng.*, 24, pp. 337-357.

12. Copyright notice

The authors are the only responsible for the printed material included in this paper.